Citation for published version:
De Simone, ME, Ciampa, F & Meo, M 2019, A hierarchical impact force reconstruction method for Aerospace composites. in *Key Engineering Materials: Advanced Materials for Defense.* vol. 812, Scientific.net, pp. 17-24. https://doi.org/10.4028/www.scientific.net/KEM.812.17

DOI:
10.4028/www.scientific.net/KEM.812.17

Publication date:
2019

Document Version
Peer reviewed version

Link to publication

University of Bath

Alternative formats
If you require this document in an alternative format, please contact:
openaccess@bath.ac.uk

General rights
Copyright and moral rights for the publications made accessible in the public portal are retained by the authors and/or other copyright owners and it is a condition of accessing publications that users recognise and abide by the legal requirements associated with these rights.

Take down policy
If you believe that this document breaches copyright please contact us providing details, and we will remove access to the work immediately and investigate your claim.

Download date: 06. May. 2023

A hierarchical impact force reconstruction method for Aerospace composites

Mario Emanuele DE SIMONE[1,a*], Francesco CIAMPA[2,b], Michele MEO[3,c]

[1,2,3] Department of Mechanical Engineering, University of Bath, Bath, United Kingdom

[a] m.e.de.simone@bath.ac.uk, [b] f.ciampa@bath.ac.uk, [c] m.meo@bath.ac.uk

Keywords: Impact force reconstruction, time reversal, radial basis functions, composite materials.

ABSTRACT

This research work presents a hierarchical method able to reconstruct the time history of the impact force on a composite wing stringer-skin panel by using the structural responses measured by a set of surface bonded ultrasonic transducers. Time reversal method was used to identify the impact location by the knowledge of structural responses recorded from a set of excitation points arbitrarily chosen on the plane of the structure. A radial basis function interpolation approach was then used to calculate the transfer function at the impact point and reconstruct the impact force history. Experimental results showed the high level of accuracy of the proposed impact force reconstruction method for a number of low-velocity impact sources and energies.

1 INTRODUCTION

Composite materials present excellent mechanical properties such as high stiffness and lightweight so that are nowadays used in many industrial applications. However, low-velocity impacts can generate micro-cracks and barely visible

damage in structures, thus leading to serious and dangerous consequences. Structural Health Monitoring (SHM) techniques have been developed in the last decades to localise the impact source [1-6] and reconstruct the force history [7-12]. A number of researches provided the force reconstruction by using the so-called "inverse approach", based on the resolution of a well-known ill-posed deconvolution problem in time domain [8]. Another approach for reconstruction of the time history of the impact force is based on artificial neural network (ANN). Such a method, however, involves the training of complex mathematical models, which makes this technique still cumbersome for real applications.

The impact force reconstruction algorithm proposed in this paper was divided in two stages. The first one relies on the impact localisation with time reversal method [4, 5], which is based on the knowledge of structural responses measured on a set of excitation points (also called "calibration points") on the plane of the specimen. At the end of this stage the "impact cell", that is the cell including the unknown impact, is identified and the location of the impact source in this cell is calculated.

The second stage consists of the impact force reconstruction, obtained following three steps: i) the calculation of the frequency response functions (reported as "transfer functions" in this work) at the corners of the impact cell by using a method able to preserve both signal modules and phases [10] at different impact energies, ii) the calculation of the transfer function at impact location by using the radial basis function (RBF) interpolation method [13] and iii) the impact force reconstruction in the time domain.

This paper builds on from the work recently published by De Simone and Ciampa [12]. The main novelty of this work is the using of a so-called "standard baseline" for recovering the impact force generated by an "unknown" source. This new baseline information corresponds to an average of the data obtained through a steel impactor generating the same impulse at each calibration points for each energy level. Other important novelties in the proposed paper are: 1) calibration points are more far away from each other with respect to the experimental tests reported in [12], therefore less baseline information was available and less impact tests were performed (quicker calibration process) considering the same monitoring area, and,

more importantly, 2) the considered specimen is not a simple plate as in [12] but a composite wing stringer-skin panel, therefore a very complex real aeronautical structure. The presented method provided high level of accuracy in the reconstruction of impact force, also if an impact source completely different from the impactor used in the initial calibration process is considered.

2 FIRST STAGE – IMPACT SOURCE LOCALISATION BY USING TIME REVERSAL METHOD

The first stage of the presented algorithm is achieved by using the time reversal (TR) method. TR is based on the hypothesis of time invariance and spatial reciprocity of elastodynamic wave equation, and the Huygens' principle, through which it is possible to reconstruct the wave function in a generic volume by the knowledge of its sources located on a two-dimensional surface [4, 5].

The aim of the first step of TR method, called "forward propagation step", consists of acquiring and storing: 1) the low-velocity impacts time histories (input signals), performed at M excitation (calibration) points on the specimen surface (focusing plane) and acquired by using a hand-held instrumented hammer, and 2) the structural responses (output signals), acquired by N receiving sensors. It should be noted that excitation points are the corners of a set of cells arranged in a grid that covers the monitoring zone of the specimen surface.

During the second step, called "backward propagation step", a correlation between the N responses due to an impact of unknown location ($G\boldsymbol{r}_{m0}$) and the $N \times M$ stored responses ($G\boldsymbol{r}_{m}$), is performed. The cross-correlation operation produces $n \times m$ functions, called "time reversal operators" $\left(R_{TR_s}\right)$. Considering the responses acquired by a single transducer, the moduli of the $1 \times M$ calculated R_{TR_s} are normalised respectively with the geometric mean between the energy of the unknown impact response $\left(E_{G\boldsymbol{r}_{m0}}\right)$, and the M energies of the stored impact responses $\left(E_{G\boldsymbol{r}_{m}}\right)$. The correlation coefficient c_{TR} is used as the similarity measurement between each presented signal couple and it is defined as:

$$c_R = max\left(\frac{|R_{TR}|}{\sqrt{E_{Gr_m}\, E_{Gr_{m0}}}}\right). \quad (1)$$

It is possible to demonstrate that Eq. (1) satisfies the inequality $0 \leq c_{TR} \leq 1$, therefore the c_{TR} is close to one when the signals are similar (i.e. at the true impact location), whilst it is close to zero elsewhere. A number of N correlation coefficients are available at each excitation point, so, in order to consider an average from the contribution of the N receiving sensors, a single mean correlation coefficient at each grid note is calculated. A further mean among the four coefficients related to the corners of each cell is performed, therefore a unique global correlation coefficient c_{TR_GLOBAL} is calculated for each cell. The impact cell is identified as the cell with the maximum c_{TR_GLOBAL}.

The coordinates of the impact source, x_I and y_I, are estimated by a centre-of-gravity method [11, 12]:

$$x_I = \frac{\sum_{i=1}^{4} x_i\, c_{TR_i}}{\sum_{i=1}^{4} c_{TR_i}}, \qquad y_I = \frac{\sum_{i=1}^{4} y_i\, c_{TR_i}}{\sum_{i=1}^{4} c_{TR_i}}, \quad (2)$$

where x_i and y_i are the coordinates of the i^{th} node of the impact cell and c_{TR_i} is the averaged correlation coefficient related to the i^{th} node.

3 SECOND STAGE – IMPACT FORCE RECONSTRUCTION

This study concerns composite components subject to low-velocity impacts. If the structure deformation is considered linearly elastic and small enough to neglect geometric nonlinearities, the relationship between an impact force $p(t)$ and the structural response $u(t)$ can be described by a linear convolution. Such time convolution corresponds to a simple product of signal spectra in the frequency domain according to the following convolution theorem:

$$u(t) = (G \otimes p)(t) = \int_0^t G(t-\tau)\, p(\tau)\, d\tau \Rightarrow U(f) = H(f) \cdot P(f)$$
$$\Rightarrow P(f) = \frac{U(f)}{H(f)} \Rightarrow p(t) = \mathcal{F}^{-1}\{P(f)\}, \tag{3}$$

where $G(t)$ is the Green function, also called "impulse response" if the excitation function is a Dirac delta function (unit impulse function), and $H(f)$ is its Fourier transform, correspondent to the frequency response function (FRF) and called "transfer function". The principal aim of this paper is to recover the spectrum of an unknown impact, and therefore the impact time history through the Inverse Fourier Transform, by the knowledge of structural responses recorded by the N receiving sensors. Information related to the transfer functions are also necessary, so input-output data acquired and stored in the first stage of the algorithm (initial calibration process) are useful in order to calculate the transfer functions on a set of calibration points (e.g. the four corners of the identified impact cell). The transfer function at impact location can be easily estimated by using a suitable interpolation method, as reported in the following Section.

3.1 TRANSFER FUNCTION CALCULATION

Transfer functions are calculated experimentally, as showed in Eq. (4) considering the i^{th} frequency component:

$$H(f_i) = \frac{S_{up}(f_i)}{S_{pp}(f_i)}, \tag{4}$$

where S_{up} is the cross-spectrum between the acquired response and the impact force and S_{pp} is the auto-spectrum of the impact force. This method is described in detail in [10]. A number of N transfer functions are available at each calibration point.

3.2 RADIAL BASIS FUNCTION INTERPOLATION

In a recent work, the authors demonstrated that hierarchical radial basis functions (RBFs) provide high accuracy in the data reconstruction when information related to a point on the structure is not available [12]. In the proposed paper, the unknown data are the N transfer functions at impact location. The RBF interpolation method, explained in detail in [13], requires the coordinates of the impact source, calculated in the first stage by using Eq. (2), and a set of data to be interpolated. These data are the coordinates of a set of calibration points and the transfer functions related to the same points and calculated by using Eq. (4). The transfer function at the impact location considering the i^{th} frequency component is calculated by using the following augmented RBF interpolant considering a two-dimensional approach:

$$h(x_I, y_I)|_{f_i} = \sum_{j=1}^{M'} \lambda_j \, \phi\left(\sqrt{\left(x_I - x_j\right)^2 + \left(y_I - y_j\right)^2}\right) + \gamma_o + \gamma_1 x_I + \gamma_2 y_I \,, \tag{5}$$

where x_I and y_I are coordinates of the impact source, x_j and y_j are coordinates of the M' arbitrary chosen calibration points (whose related information needs to be interpolated), λ_j and γ_k are the expansion coefficients and $\phi(\cdot)$ is a suitable radial basis function. The expansion coefficients are calculated as shown below, as solutions of a linear system of equations:

$$\begin{bmatrix} \lambda_1 \\ \vdots \\ \lambda_{m'} \\ \gamma_1 \\ \gamma_2 \\ \gamma_o \end{bmatrix} = \begin{bmatrix} \phi_{1,1} & \cdots & \phi_{1,m'} & x_1 & y_1 & 1 \\ \vdots & \ddots & \vdots & \vdots & \vdots & \vdots \\ \phi_{m',1} & \cdots & \phi_{m',m'} & x_{m'} & y_{m'} & 1 \\ x_1 & \cdots & x_{m'} & 0 & 0 & 0 \\ y_1 & \cdots & y_{m'} & 0 & 0 & 0 \\ 1 & \cdots & 1 & 0 & 0 & 0 \end{bmatrix}^{-1} \begin{bmatrix} h_1|_{f_i} \\ \vdots \\ h_{m'}|_{f_i} \\ 0 \\ 0 \\ 0 \end{bmatrix}, \tag{6}$$

where $h_1|_{f_i} \ldots h_{m'}|_{f_i}$ are the values of the transfer functions related to the M' arbitrary chosen calibration points at the i^{th} frequency component. The thin plate spline (TPS) is used as radial basis function [12], whose kernel is $\phi(\cdot) = (\cdot)^2 \, ln(\cdot)$.

The described process is performed N times (i.e. N transfer functions are available at each considered point) for all the frequency range. At the end of this step, a number of N transfer functions are available at the impact location.

3.3 IMPACT FORCE IDENTIFICATION

Once the transfer functions at the impact location are obtained, n simple divisions, component by component, are performed, as showed in Eq. (3). Such division allows obtaining N impact spectra, whose their mean is the final impact spectrum, as performed in [11, 12]. The inverse Fourier Transform of the calculated impact spectrum represents the time histories of the unknown impact event. In this paper, the final impact spectrum is obtained by using a different approach, that is the same developed in [7, 10] to take in account the measurements coming from the N receiving sensors. Such approach is shown below:

$$P(f) = \sum_{i=0}^{n} \left[\frac{H_{S_1}^{*}\, U_{S_1} + H_{S_2}^{*}\, U_{S_2} + \cdots + H_{S_n}^{*}\, U_{S_n}}{\left|H_{S_1}\right|^2 + \left|H_{S_2}\right|^2 + \cdots + \left|H_{S_n}\right|^2 + R} \right]_{f_i} \Rightarrow$$

$$\Rightarrow p(t) = \mathcal{F}^{-1}\{P(f)\}\,. \tag{7}$$

The subscripts $S_1, \ldots, S_n$ refer to the N receiving sensors, f_i indicates the frequency component, H^* and $|H|^2$ represents respectively the complex conjugate and the square of the complex modulus of the transfer function. R represents a small amount of random noise, necessary to avoid division by zero in Eq. (3). Experimental tests demonstrated the higher accuracy of the reconstructed impact force by using the described method [Eq. (7)] compared to the approach followed by the authors in [12].

4 EXPERIMENTAL SET-UP

In order to validate the described algorithms, experimental impact tests were conducted on a composite wing stringer-skin panel provided by the courtesy of Airbus UK, with average dimensions of $1680 \times 708 \times 27$ mm^3 (see Figure 1).

The impacts were generated by using a hand-held instrumented hammer (sensitivity factor $= 2.215$ mV/N) connected to a signal conditioner, both manufactured by Meggit-Endevco. Two tips with different hardness were investigated: the steel one was adopted in the initial calibration process, whilst the softer rubber one was used for the unknowns impacts. The calibration process was performed through five impacts with maximum amplitudes at 180 N and five impacts with maximum amplitudes at 270 N, at each calibration point (see Figure 2a), whilst the unknown impacts were performed by using the instrumented hammer connected to a pendulum-system, dropping five times from two different heights (see Figure 2b). Three acoustic emission transducers with 300 kHz central frequency provided by Airbus UK were chosen and arranged in a triangular shape backward the focusing plane (see Figure 1b and Figure 1c). The monitoring area consists of a grid arranged with equally spaced nodes (30 mm), which are the calibration points (see Figure 1a). Signals were acquired using a four-channel oscilloscope with 16 bits of resolution, a sampling rate of 1 MHz and an acquisition window of 10 ms. All algorithms were implemented by the authors by using a MATLAB software code.

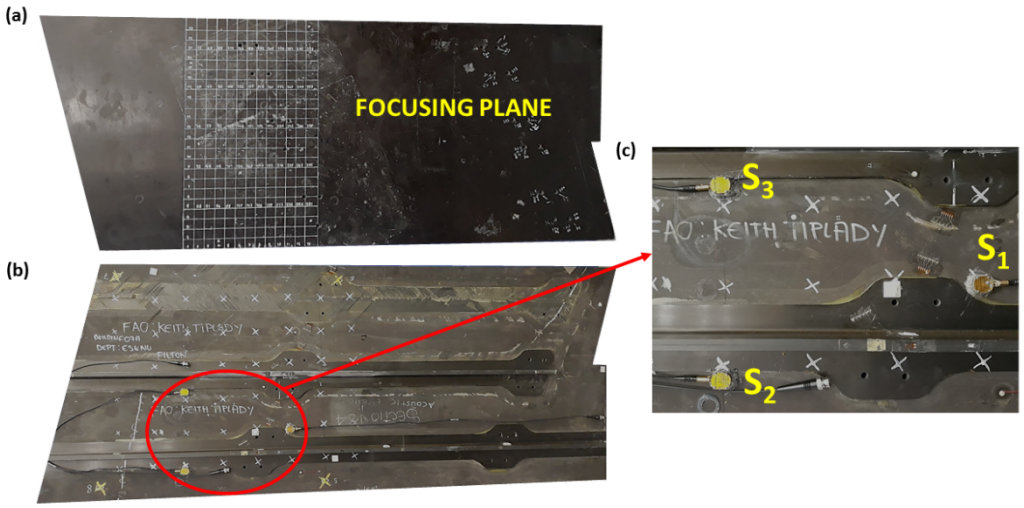

Figure 1. Composite wing stringer-skin panel: focusing plane (a); backward part of the specimen (b); zoom on the transducer locations (c).

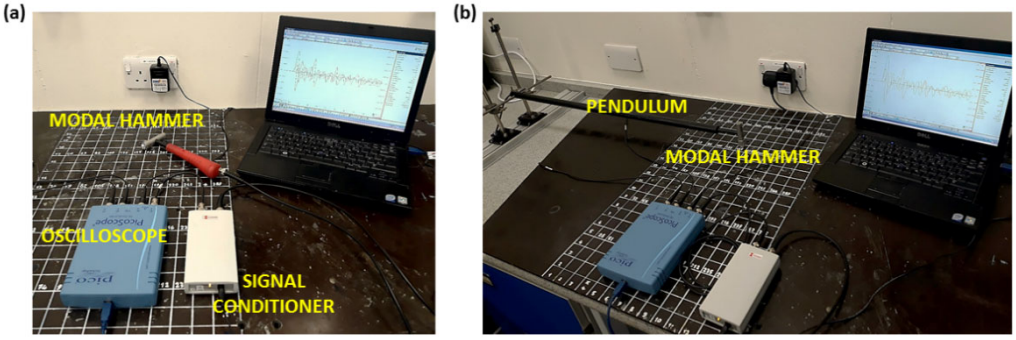

Figure 2. Experimental set-up for: baseline data acquisition (a) and unknown impacts data acquisition (b).

5 RESULTS

Experimental tests revealed that the accuracy of the presented algorithm is guaranteed at each point of the monitoring zone. For clarity reasons, experimental results on ten impacts occurred at the centre of the monitoring zone (see Figure 3) are shown in this Section. The two energy levels considered for the unknown impacts led maximum peak amplitudes at around 180 N and 270 N.

The accuracy of the force reconstruction algorithm is expressed by considering two error functions: the first one [Eq. (8)] represents an error based on time integral of the force in an interval of the recording $[t_2 - t_1]$ which includes the impact force [10, 12]. The second error function [Eq. (8)] estimates the percentage error of the reconstructed impact peak amplitudes with respect to the actual ones [11]. It should be noted that time histories of unknown impacts are available by means of the recorded instrumented hammer data, which was connected to the pendulum-system.

$$a) \quad \Gamma_1 = \frac{\int_{t_1}^{t_2} |p_{real}(t) - p_{rec}(t)|\, dt}{\int_{t_1}^{t_2} p_{real}(t)\, dt}\,, \qquad b) \quad \Gamma_2 = \frac{|max(amp)_{real} - max\ (amp)_{rec}|}{max(amp)_{real}} \times 100\%\,. \tag{8}$$

Figure 3 depicts the monitoring zone of the composite wing with dimensions of 210×330 mm^2: the red "plus" marks indicate transducer locations, the blue "dot" marks represent the calibrations points and the four red "dot" marks are the corners of the impact cell (cell 155), identified with TR method.

Impacts performed at cell 155 (see green mark in Figure 3), generated by the instrumented hammer, were identified by the localisation algorithm with high level of accuracy, with an error always less than 5 mm. The expression for the location error is reported below [6]:

$$\Psi = \sqrt{(x_{real} - x_{calculated})^2 + (y_{real} - y_{calculated})^2}\,, \tag{9}$$

where (x_{real}, y_{real}) are the coordinates of the true impact position and $(x_{calculated}, y_{calculated})$ are the coordinates of the impact location calculated by using Eq. (2).

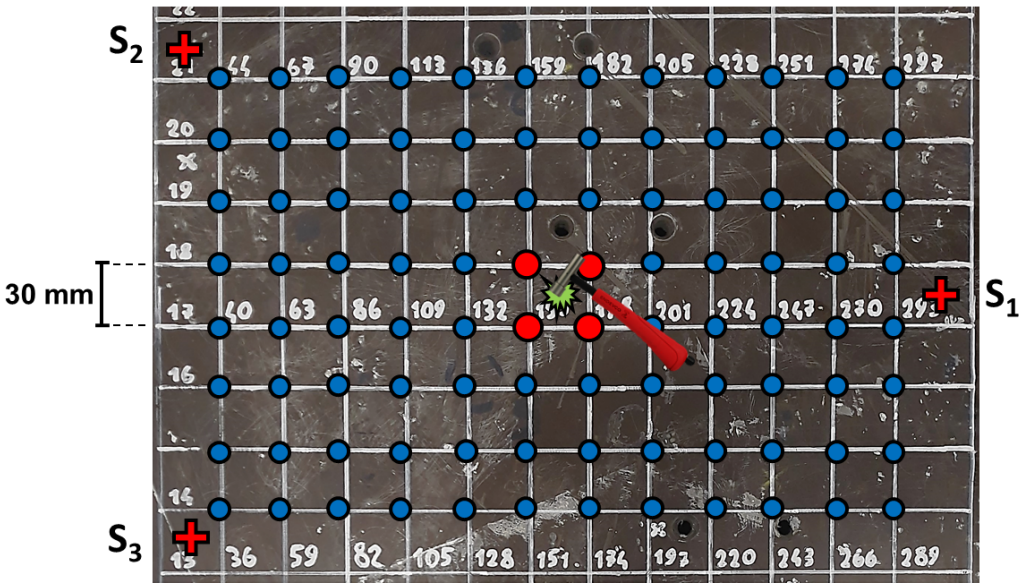

Figure 3. Zoom on the monitoring zone of the composite wing. Transducer locations, calibration points and impact cell are reported. The green mark represents the unknown impact at cell 155.

Once identified the impact source location and the impact cell, the two baseline data sets (at 180 N and 270 N) related to the four corners were extrapolated, averaged and used for the RBF interpolation.

Three transfer functions related to the impact location were available at the end of the interpolation process, due to the contribution of the three receiving sensors. The mean impact spectrum and the time history of the impact force were obtained by using Eq. (7).

In Figure 4 and Figure 5, the reconstruction of ten unknown impacts with maximum amplitudes respectively at around 180 N and 270 N are presented. The considered time interval for the Γ_1 error [Eq. (8a)] was $t_1 = 0.5$ ms and $t_2 = 1.6$ ms. As depicted in figures below the unknown impact forces were reconstructed with high accuracy, with a maximum difference in peak amplitudes less than 1.1% for the first set of impacts (180 N) and less than 2.2% for the second set (270 N).

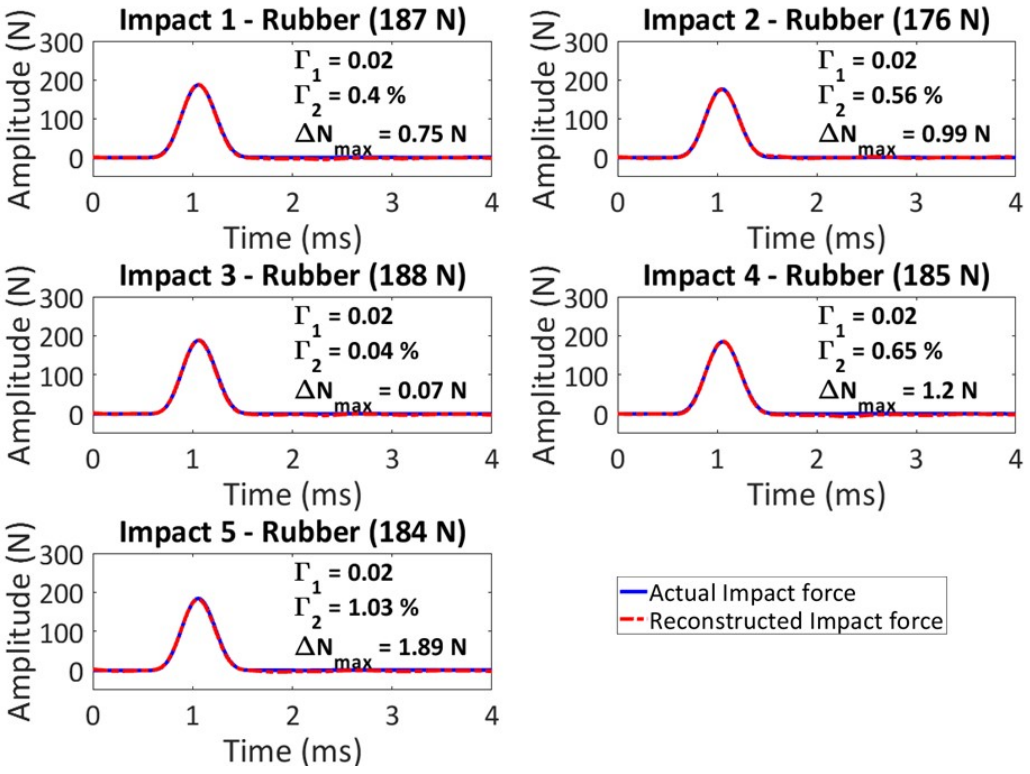

Figure 4. Reconstruction of the first set of unknown impact forces with error comparison values. The five impacts were recorded by the instrumented hammer with the rubber tip. The maximum peak amplitudes were at around 180 N.

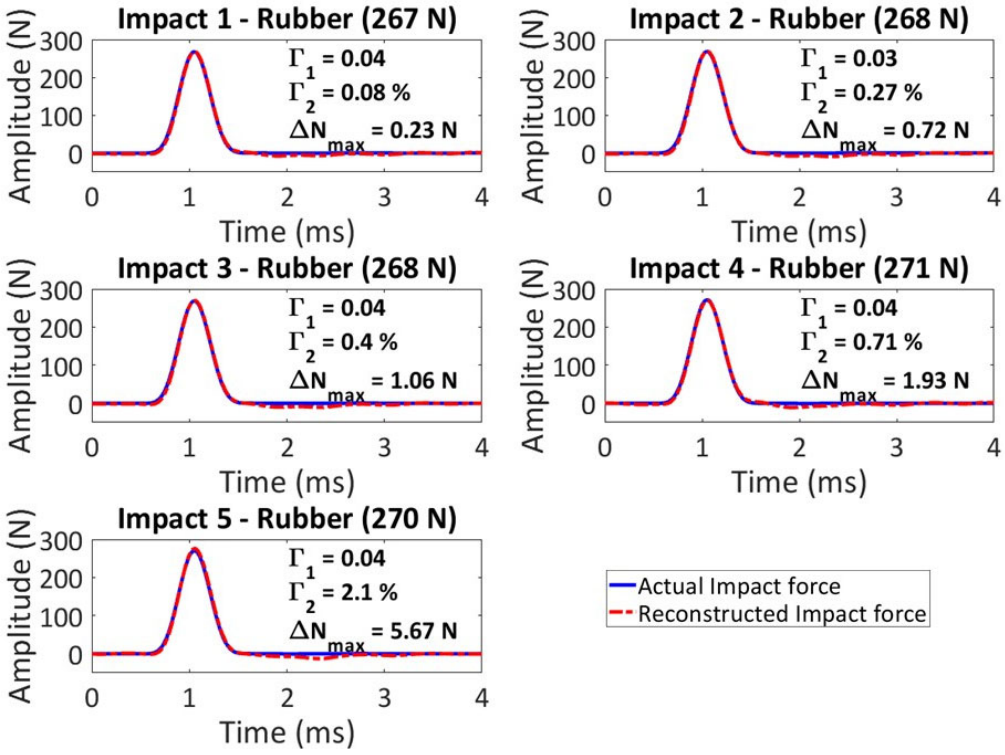

Figure 5. Reconstruction of the second set of unknown impact forces with error comparison values. The five impacts were recorded by the instrumented hammer with the rubber tip. The maximum peak amplitudes were at around 270 N.

6 CONCLUSIONS

A method capable of reconstructing the impact force due to low-velocity impacts was presented and investigated. The localisation of the source events was performed by using the time reversal method, therefore an initial calibration process was necessary. It consists of acquiring and storing impact forces with different peak amplitudes and structural responses, recorded by using respectively a hand-held instrumented hammer and a set of surface bonded ultrasonic transducers, from a set of excitation points on the specimen's surface. Transfer functions at the four corners of the identified impact cell were calculated, averaged and interpolated by using a hierarchical radial basis function algorithm. The mean impact spectrum and impact force were calculated. A number of experimental tests was performed on a composite wing stringer-skin panel in order to validate the proposed methodology.

The algorithm was able to reconstruct impact forces due to object different with respect to the impactor used in the calibration process with high accuracy. The error functions showed a negligible difference between the actual impact forces and the reconstructed ones.

REFERENCES

1. Meo, M., Zumpano, G., Piggott, M., & Marengo, G. (2005). Impact identification on a sandwich plate from wave propagation responses. *Composite structures*, *71*(3-4), 302-306.
2. Ciampa, F., Meo, M., & Barbieri, E. (2012). Impact localization in composite structures of arbitrary cross section. *Structural Health Monitoring*, *11*(6), 643-655.
3. Kundu, T. (2014). Acoustic source localization. *Ultrasonics*, *54*(1), 25-38.
4. Ciampa, F., & Meo, M. (2014). Impact localization on a composite tail rotor blade using an inverse filtering approach. *Journal of Intelligent Material Systems and Structures*, *25*(15), 1950-1958.
5. Ciampa, F., Boccardi, S., & Meo, M. (2016). Factors affecting the imaging of the impact location with inverse filtering and diffuse wave fields. *Journal of Intelligent Material Systems and Structures*, *27*(11), 1523-1533.
6. De Simone, M. E., Ciampa, F., Boccardi, S., & Meo, M. (2017). Impact source localisation in aerospace composite structures. *Smart Materials and Structures*, *26*(12).
7. Martin, M. T., & Doyle, J. F. (1996). Impact force identification from wave propagation responses. *International journal of impact engineering*, *18*(1), 65-77.
8. Jacquelin, E., Bennani, A., & Hamelin, P. (2003). Force reconstruction: analysis and regularization of a deconvolution problem. *Journal of sound and vibration*, *265*(1), 81-107.
9. Park, J., Ha, S., & Chang, F. K. (2009). Monitoring impact events using a system-identification method. *AIAA journal*, *47*(9), 2011-2021.
10. Thiene, M., Ghajari, M., Galvanetto, U., & Aliabadi, M. H. (2014). Effects of the transfer function evaluation on the impact force reconstruction with application to composite panels. *Composite Structures*, *114*, 1-9.
11. Xu, L., Wang, Y., Cai, Y., Wu, Z., & Peng, W. (2016). Determination of impact events on a plate-like composite structure. *The Aeronautical Journal*, *120*(1228), 984-1004.
12. De Simone, M. E., Ciampa, F., & Meo, M. (2019). A hierarchical method for the impact

force reconstruction in composite structures. *Smart Materials and Structures*, *28*(8).

13. Wright, G. B. (2003). Radial basis function interpolation: numerical and analytical developments. University of Colorado, Boulder, Doctoral dissertation.